ThermoFisher
SCIENTIFIC

Cell sorting

Bigfoot Cell Sorter using 28-color panel sorts with high efficiency, purity, and recovery

Keywords

Bigfoot cell sorter, cell sorting, spectral unmixing, flow cytometry, high-parameter panel

Introduction

The demand for higher-parameter multicolor data in flow cytometry has amplified interest in spectral data unmixing and analysis as compared to the traditional method of compensation for fluorescence spillover. Investigators frequently find it challenging to resolve dim, rare, or highly autofluorescent populations or high-parameter panels using standard compensation. Although some cytometric systems offer post-acquisition spectral unmixing, workflows can be challenging, and experiments may consume a larger volume of controls and precious sample for setup. To improve usability, the Invitrogen™ Bigfoot™ Cell Sorter provides innovative hardware and software that gathers full-spectrum data and then sorts cells using spectrally unmixed data in real time.

Here we use a 28-color mouse immunophenotyping panel to demonstrate the spectral unmixing and sorting capability of the Bigfoot Cell Sorter to resolve fluorescent signals accurately and precisely, sort six ways simultaneously with great efficiency, and produce highly pure sorted samples. We present application data that demonstrate sufficient resolution for accurate gating needed in studies involving immunophenotyping and marker expression. We also provide post-sort efficiency, purity, and recovery data obtained on the Invitrogen™ Attune™ NxT Flow Cytometer.

28-color immunophenotyping panel

Importance of high-parameter panels

Immunophenotyping panels are used to identify, characterize, and categorize cellular subsets within a sample using flow cytometry. This is done by detecting signals from fluorophores that are coupled to antibodies that bind to specific antigens expressed by the cells. In the past, an investigator would need to run parallel panels on the same cell sample to determine the phenotypes of cellular subsets. Each panel required additional reagent and sample, which incurred expense, wasted sample, and resulted in increased instrument run time. Another disadvantage of using separate panels is that potential co-expression of markers or additional subset identification is not detected. For example, in mice the Ly6C marker is routinely used to identify monocytes/macrophages and granulocytes and might not be included in panels for studying T cells by investigators who are not familiar with this field. Therefore, the characterization of CD4 and CD8 T cells expressing Ly6C in different biological contexts is hampered compared to the study of more commonly used T cell markers, restricting overall understanding of immune system function. However, the Bigfoot Cell Sorter can now facilitate complex immunophenotyping with one optimized 28-color panel. When more parameters are analyzed from a single sample, further enumeration of cell subsets can be determined more efficiently.

invitrogen

Panel design

This broad 28-color immunophenotyping panel identifies immunologically relevant populations present in lymphoid organs of general interest to the scientific community and was created following basic panel-building precepts. The main principle of good panel design is to distribute the fluorophores over the spectral range, which is defined by the number of lasers and detectors available on the instrument, to minimize panel complexity and fluorophore spread. A spectral panel design grid (Table 1) provides a straightforward way to visualize potential fluorophore overlap. To build a spectral panel design grid, list available lasers in different columns and then list the channels associated with each laser in rows. Include each fluorophore–antigen pair in the grid at its emission peak. This arrangement helps to visualize where two or more fluorophores could have overlapping signals, based on their proximity to the same column or row of the grid.

Table 1. 28-color immunophenotyping panel for a 6-laser Bigfoot Cell Sorter experiment.

UV 349		V 405		VB 445		B 488		Y 561		R 640	
Channel	Antigen and fluorophore	Channel	Antigen and fluorophore	Channel	Antigen and fluorophore	Channel	Antigen and fluorophore	Channel	Antigen and fluorophore	Channel	Antigen and fluorophore
UV1 387/11	CD25 Brilliant Ultra Violet 395	V1 420/10	Siglec-H Brilliant Violet 421								
UV2 420/10											
UV3 434/17		V2 434/17									
UV4 455/14		V3 455/14	CD21 eFluor 450								
				VB1 465/22	CD62L Brilliant Violet 480						
UV5 473/15		V4 473/15									
UV6 507/19	CD19 Brilliant Ultra Violet 496	V5 507/19	CCR2 Brilliant Violet 510			B1 507/19	TER-119 FITC				
				VB2 525/36							
UV7 549/15		V6 549/15				B2 549/15	LIVE/DEAD Fixable Olive				
UV8 575/15	CD44 Brilliant Ultra Violet 563	V7 575/15	CD8 Brilliant Violet 570					Y1 575/15	CD127 PE		
				VB3 583/30		B3 583/30		Y2 589/15			
								Y3 605/15	IgM PE-eFluor 610		
UV9 615/24	CD11c Brilliant Ultra Violet 615	V8 615/24	I-A/I-E Super Bright 600			B4 615/24					
								Y4 625/15			
				VB4 650/LP							
		V9 661/20	Ly6G Brilliant Violet 650					Y5 661/20	CD3 PE-Cy5		
UV10 670/30	CD93 Brilliant Ultra Violet 661					B5 670/30				R1 670/30	CD335 (Nkp46) APC
								Y6 685/15			
								Y7 700/13		R2 700/13	CD45 NovaFluor Red 700
		V10 710/20	IgD Super Bright 702								
UV11 728/40						B6 720/60	CD1d PerCP-eFluor 710	Y8 720/24	CD49b PE-Cy5.5	R3 720/24	
		V11 747/33	CD4 Brilliant Violet 750							R4 760/50	
UV12 750/LP	B220 Brilliant Ultra Violet 805	V12 770/LP	CD11b Super Bright 780			B7 750/LP	CD24 RealBlue 780	Y9 760/50	CD23 PE-Cy7		
										R5 770/LP	Ly6C APC-eFluor 780
								Y10 800/12			
								Y11 832/37			
								Y12 860/LP			

Bigfoot Cell Sorter   thermofisher.com/bigfoot

When two fluorophores are far apart in the grid the potential overlap between them is low. However, when two fluorophores are close together in the grid, either within the same column or within the same row, their overlap potential is higher. The loss of resolution that can result from fluorophore spread can then be mitigated by matching antigen density to fluorophore brightness while considering co-expression of these antigens in different cell subsets.

An additional tool for ensuring the success of a spectral panel is to generate a similarity matrix and complexity index for the proposed panel (Figure 1). The spectral similarity matrix will consider the instrument's lasers and detectors and provide a quantitative approximation of fluorophore similarity on the chosen instrument configuration. The complexity index considers all the overlapping signals present in a panel. These tools, along with the spectral panel grid, help investigators to distribute fluorophores among different detectors and lasers to mitigate the effects of co-expression. This provides some redundancy, in an easy-to-read display that can help investigators select fluorophore combinations that reduce panel complexity. It is also important to note that neither complexity scores nor panel design matrices consider fluorophore brightness. Matching antigen density to fluorophore brightness is another way to achieve optimal data resolution.

Complexity Index: 5.40
⌄ Spectral Matrix

Spectral Similarity Matrix   Low ▇▇▇▇ High

	BUV 395	BUV 496	BUV 563	BUV 615	BUV 661	BUV 805	BV 421	eFluor 450	BV 480	BV 510	BV 570	SuperBright 600	BV 650	SuperBright 702	BV 750	SuperBright 780	FITC	LIVE-DEAD Fixable Olive 557	PerCP-eFluor 710	Real Blue 780	PE	PE-eFluor 610	PE-Cy5	PE-Cy5.5	PE-Cy7	APC	NovaRed 700	APC-eFluor 780
BUV 395		0.09	0.12	0.10	0.16	0.15	0.14	0.06	0.01	0.04	0.02	0.01	0.03	0.06	0.01	0.02	0.00	0.00	0.00	0.00	0.00	0.00	0.00	0.00	0.00	0.00	0.00	0.00
BUV 496	0.09		0.28	0.06	0.03	0.02	0.03	0.04	0.21	0.49	0.04	0.02	0.01	0.02	0.01	0.01	0.13	0.04	0.00	0.00	0.01	0.01	0.00	0.01	0.00	0.00	0.00	0.00
BUV 563	0.12	0.28		0.34	0.10	0.02	0.02	0.01	0.03	0.26	0.20	0.09	0.04	0.02	0.01	0.00	0.06	0.04	0.01	0.00	0.11	0.07	0.02	0.03	0.04	0.00	0.00	0.00
BUV 615	0.10	0.06	0.34		0.36	0.06	0.02	0.01	0.01	0.11	0.14	0.23	0.16	0.05	0.03	0.02	0.01	0.01	0.04	0.01	0.06	0.16	0.06	0.04	0.03	0.01	0.00	0.02
BUV 661	0.16	0.03	0.10	0.36		0.22	0.03	0.01	0.01	0.04	0.04	0.07	0.28	0.16	0.12	0.06	0.00	0.01	0.13	0.03	0.01	0.02	0.16	0.12	0.04	0.18	0.13	0.13
BUV 805	0.15	0.02	0.02	0.06	0.22		0.02	0.01	0.00	0.01	0.00	0.00	0.04	0.08	0.27	0.24	0.00	0.02	0.10	0.00	0.00	0.00	0.02	0.11	0.00	0.00	0.00	0.26
BV 421	0.14	0.03	0.02	0.02	0.03	0.02		0.69	0.09	0.11	0.16	0.07	0.16	0.39	0.04	0.16	0.00	0.00	0.00	0.00	0.00	0.00	0.00	0.00	0.00	0.00	0.00	0.00
eFluor 450	0.06	0.04	0.01	0.01	0.01	0.01	0.69		0.27	0.29	0.12	0.07	0.12	0.39	0.03	0.16	0.01	0.00	0.00	0.00	0.00	0.00	0.00	0.00	0.00	0.00	0.00	0.00
BV 480	0.01	0.21	0.03	0.01	0.01	0.00	0.09	0.27		0.59	0.07	0.05	0.03	0.08	0.01	0.03	0.27	0.25	0.01	0.00	0.01	0.00	0.00	0.00	0.01	0.00	0.00	0.00
BV 510	0.04	0.49	0.26	0.11	0.04	0.01	0.11	0.29	0.59		0.36	0.24	0.13	0.10	0.01	0.04	0.15	0.17	0.01	0.00	0.02	0.02	0.01	0.01	0.01	0.00	0.00	0.00
BV 570	0.02	0.04	0.02	0.14	0.04	0.00	0.16	0.12	0.07	0.36		0.66	0.30	0.12	0.02	0.04	0.04	0.17	0.02	0.00	0.28	0.21	0.06	0.06	0.09	0.01	0.00	0.01
SuperBright 600	0.01	0.02	0.09	0.23	0.07	0.00	0.07	0.07	0.05	0.24	0.66		0.55	0.11	0.02	0.02	0.01	0.10	0.02	0.00	0.11	0.20	0.06	0.04	0.04	0.01	0.01	0.00
BV 650	0.03	0.01	0.04	0.16	0.28	0.04	0.16	0.12	0.03	0.13	0.30	0.55		0.45	0.23	0.15	0.00	0.05	0.10	0.01	0.01	0.05	0.12	0.08	0.03	0.07	0.07	0.05
SuperBright 702	0.06	0.02	0.02	0.05	0.16	0.08	0.39	0.39	0.08	0.10	0.12	0.11	0.45		0.46	0.34	0.00	0.01	0.12	0.02	0.00	0.00	0.03	0.11	0.03	0.04	0.13	0.07
BV 750	0.01	0.01	0.01	0.03	0.12	0.27	0.04	0.03	0.01	0.01	0.02	0.02	0.23	0.46		0.84	0.00	0.01	0.08	0.08	0.00	0.00	0.01	0.07	0.10	0.01	0.04	0.16
SuperBright 780	0.02	0.01	0.00	0.02	0.06	0.24	0.16	0.16	0.03	0.04	0.04	0.02	0.15	0.34	0.84		0.00	0.01	0.04	0.08	0.00	0.00	0.00	0.03	0.11	0.00	0.01	0.15
FITC	0.00	0.13	0.06	0.01	0.00	0.00	0.00	0.01	0.27	0.15	0.04	0.01	0.00	0.00	0.00	0.00		0.50	0.01	0.00	0.07	0.09	0.02	0.07	0.00	0.00	0.00	0.00
LIVE-DEAD Fixable Olive	0.00	0.04	0.04	0.01	0.01	0.00	0.00	0.00	0.25	0.17	0.17	0.10	0.05	0.01	0.01	0.01	0.50		0.13	0.03	0.41	0.27	0.09	0.10	0.16	0.00	0.00	0.01
PerCP-eFluor 710	0.00	0.00	0.01	0.04	0.13	0.02	0.00	0.00	0.01	0.01	0.02	0.02	0.10	0.12	0.08	0.04	0.01	0.13		0.15	0.02	0.06	0.37	0.77	0.19	0.07	0.09	0.05
Real Blue 780	0.00	0.00	0.00	0.01	0.03	0.10	0.00	0.00	0.00	0.00	0.00	0.00	0.01	0.02	0.08	0.08	0.00	0.03	0.15		0.00	0.01	0.02	0.11	0.66	0.00	0.00	0.08
PE	0.00	0.01	0.11	0.06	0.01	0.00	0.00	0.00	0.01	0.02	0.28	0.11	0.01	0.00	0.00	0.00	0.17	0.41	0.02	0.00		0.56	0.12	0.14	0.30	0.02	0.00	0.00
PE-eFluor 610	0.00	0.01	0.07	0.16	0.02	0.00	0.00	0.00	0.00	0.02	0.21	0.20	0.05	0.00	0.00	0.00	0.09	0.27	0.06	0.01	0.56		0.23	0.13	0.18	0.05	0.01	0.01
PE-Cy5	0.00	0.00	0.02	0.06	0.16	0.00	0.00	0.00	0.00	0.01	0.06	0.06	0.12	0.03	0.01	0.00	0.02	0.09	0.37	0.02	0.12	0.23		0.42	0.68	0.57	0.25	0.08
PE-Cy5.5	0.00	0.00	0.03	0.04	0.12	0.02	0.00	0.00	0.00	0.01	0.06	0.04	0.08	0.11	0.07	0.03	0.10	0.10	0.77	0.11	0.14	0.13	0.42		0.31	0.21	0.33	0.11
PE-Cy7	0.00	0.01	0.04	0.03	0.04	0.11	0.00	0.00	0.01	0.01	0.09	0.04	0.03	0.03	0.10	0.11	0.07	0.16	0.19	0.66	0.30	0.18	0.68	0.31		0.02	0.03	0.19
APC	0.00	0.00	0.00	0.01	0.18	0.00	0.00	0.00	0.00	0.00	0.01	0.01	0.07	0.04	0.01	0.00	0.00	0.00	0.07	0.00	0.02	0.05	0.57	0.21	0.02		0.59	0.25
NovaRed 700	0.00	0.00	0.00	0.00	0.13	0.00	0.00	0.00	0.00	0.00	0.00	0.01	0.07	0.13	0.04	0.01	0.00	0.00	0.09	0.00	0.00	0.01	0.25	0.33	0.03	0.59		0.25
APC-eFluor 780	0.00	0.00	0.00	0.02	0.13	0.26	0.00	0.00	0.00	0.00	0.01	0.01	0.05	0.07	0.16	0.15	0.00	0.01	0.05	0.08	0.00	0.01	0.08	0.11	0.19	0.16	0.25	

Figure 1. Spectral similarity matrix. The spectral similarity matrix available in Invitrogen™ Sasquatch Software (SQS) allows the user to readily visualize fluorophore combinations that are significantly overlapping, as indicated here by the intensity of blue shading. For each fluorophore intersection in an "x" by "y" view, a value between 0 and 1 indicates the similarity between the pair. The use of highly similar fluorophores together directly contributes to increased panel complexity and ultimately translates to reduced resolution of target populations after unmixing. BUV: Brilliant Ultra Violet™ dye, BV: Brilliant Violet™ dye.

Sensitivity and resolution

In addition to panel design, many factors influence instrument sensitivity and population resolution. Therefore, it is important to consider the mechanical, chemical, and biological factors that impact an experiment.

Instrumentation

The Bigfoot Cell Sorter features jet-in-air sample stream interrogation and photomultiplier tubes (PMTs) for detection, while other spectral sorters use a cuvette for sample interrogation and avalanche photodiodes (APDs) for detection. There are pros and cons associated with either option. PMTs can achieve a higher signal-to-noise ratio than APDs under some circumstances, while APDs may decrease the overall cost of the instrument. When arrayed end to end across the full spectrum, using customized single-channel filters, PMTs can provide improved differentiation of the fluorophore spectra. Researchers should take into account the mechanical differences in instrument architecture, to optimize their flow cytometry panels for the specific instruments on which the panels will run. Fluorophore–antigen pairings and sample characteristics also contribute to this requirement.

The physics involved in jet-in-air sorting are also important, as this method is thought to exert less acceleration and shear force on cells during a sort. Some researchers have reported that jet-in-air sorters have minimal impact on gene expression in sorted cells [1–5]. The Flow Cytometry Research Group presented initial data in 2015 that favorably compared a jet-in-air sorter with two different sorters that feature cuvette interrogation. The report by Cochran et al. (2015) demonstrated that a jet-in-air instrument caused fewer changes in cellular gene expression compared to two cuvette models [5]. This was not a definitive study, and this area of research continues to emerge. What is clear is that researchers should always be cognizant of the mechanical characteristics of the sorter or analyzer on which their immunophenotyping panel will be run, as these play a key role in both cell physiology and fluorophore detection.

Fluorophore–antigen pairs

Each fluorophore has unique physical and chemical properties that allow it to absorb light energy and emit resonant energy as photons, resulting in a certain level of fluorophore brightness. Additionally, many fluorophore choices are available with many antibody choices, each with variable affinity for the antigen on the biological specimen. Therefore, population resolution may not be the same between biological samples, experimental conditions, or different fluorophore–antigen pairings. Panel components should always be verified on the instrument on which the assay will be run, and optimized on experimentally relevant biological samples.

Experiment setup

Bone marrow, spleen, and lymph node tissues from specific pathogen-free (SPF) BALB/c mice were processed into single-cell suspension samples, stained, and fixed for acquisition on a 6-laser Bigfoot Cell Sorter. Although data were successfully collected and analyzed with the Bigfoot Cell Sorter for all three tissue types, for this paper's purpose, most of the data shown are from the spleen sample because sorting was performed on spleen cell subsets.

The instrument was configured with 349 nm, 405 nm, 445 nm, 488 nm, 561 nm, and 640 nm lasers. The 445 nm laser is unique in its ability to excite Brilliant Violet™ 480 and PerCP-eFluor™ 710 dyes for added spectral dimension, which makes greater data resolution of these fluorophores possible even when they are used on co-expressed antigens.

A key factor for ensuring successful spectral unmixing during acquisition of controls is to minimize sample carryover between the controls. If samples or fluorophores are particularly adherent, the number or duration of wash steps between samples can be increased, which can be set automatically in Sasquatch Software.

Unmixing controls were prepared with two drops of Invitrogen™ UltraComp eBeads™ Plus Compensation Beads (Cat. No. 01-3333-42) and were incubated with 0.1 µg of antibody for 20 minutes at 4°C, protected from light. The exceptions for which either bone marrow cells or spleen cells were used are shown in Table 2. In those instances, the specified cells were used to avoid generating unmixing errors due to overall greater brightness and/or different fluorescence profiles as compared to beads.

In Sasquatch Software, a new sort workflow was selected and designated as a spectral experiment. The required fluorophores were selected, and the option to add a secondary unstained control was selected to use beads. Since both cells and beads were used in this experiment, the appropriate autofluorescent background, from either beads or cells, was chosen for each unmixing control before controls were acquired. The voltages determined by the median fluorescence intensity (MFI) automated QC process were used as the baseline, and then voltages were optimized for the panel. After the voltages were set, the single-color controls were run sequentially using the multi-sample loader. The unmixing was automatically applied, and the resulting spectral parameters then became selectable in sample plots and were used for gating in the workspace. The instrument was fitted with a 100 µm nozzle, and samples were run at 30 psi in purity sort mode.

Materials and methods

Tissue processing and dilution

Specific pathogen-free (SPF) BALB/c mice were maintained at Thermo Fisher Scientific (Carlsbad, California), with sterile water and feed provided ad libitum, per IACUC guidance. The spleen, lymph nodes, femurs, and tibias were harvested after carbon dioxide euthanasia. Single-cell suspensions were prepared from the bone marrow by flushing the bones with complete medium [Gibco™ BenchStable™ RPMI 1640 with GlutaMAX™ Supplement (Cat. No. A41923-01) supplemented with 5% heat-inactivated Gibco™ Fetal Bovine Serum (FBS) (Cat. No. A5209501) and 50 units/mL of Gibco™ Penicillin-Streptomycin (Cat. No. 15070-063)], followed by filtering the suspension with a 70 µm cell strainer. Single-cell suspensions were prepared from the spleen and lymph nodes by mechanical dissociation using the same complete medium used for the bone marrow cells, followed by filtering the suspension with a 70 µm cell strainer.

Red blood cell lysis was performed to remove most erythrocytes from splenic and bone marrow cell suspensions, using Invitrogen™ eBioscience™ 10X RBC Lysis Buffer (Cat. No. 00-4300-54) as recommended, followed by washing and incubating the cell suspension with complete medium with 100 µg/mL DNase I (Millipore-Sigma, Cat. No. 11284932001) for 15 minutes. Afterward, cell concentration and viability were assessed using an Invitrogen™ Countess™ 3 FL Automated Cell Counter (Cat. No. A49893). Cell concentration was adjusted to 1×10^7 cells/mL.

Sample staining

Cells were pre-blocked with mouse Fc receptor (BD Biosciences, Cat. No. 553142) for 5 minutes in Invitrogen™ eBioscience™ Staining Buffer (Cat. No. 00-4222-26) to prevent nonspecific binding of cells, followed by adding antibodies (Table 2) containing 5 µL/test of Invitrogen™ CellBlox™ Blocking Buffer (Cat. No. B001T03F01) and 5 µL/test of Invitrogen™ eBioscience™ Super Bright Complete Staining Buffer (Cat. No. SB-4401-42), which are used to prevent nonspecific binding and nonspecific polymer interactions, respectively. Cell staining was performed for 20 minutes at 4°C, protected from light. Staining with the Invitrogen™ LIVE/DEAD™ Fixable Olive Viability Kit (Cat. No. L34978) was performed in phosphate-buffered saline (PBS), pH 7.4, for 20 minutes at 4°C, protected from light, to distinguish live from dead and dying cells. Following incubation with the viability dye, cells were fixed in a final concentration of 2% formaldehyde (BioLegend, Cat. No. 420801) for 30 minutes at room temperature, protected from light.

Table 2. 28-color immunophenotyping panel.

Laser and channel	Filter	Fluorophore	Antigen	Clone	Titration	Unmixing control	Fluorescence-minus-one (FMO) controls	Supplier	Cat. No.
349 UV1	387/11	Brilliant Ultra Violet 395	CD25	PC61	2 µL (0.4 µg/test)	Beads	Yes	BD Biosciences	564022
349 UV6	507/19	Brilliant Ultra Violet 496	CD19	eBio1D3	2 µL (0.4 µg/test)	Mouse cells (spleen)		Thermo Fisher Scientific	364-0193-82
349 UV8	575/15	Brilliant Ultra Violet 563	CD44	IM7	0.8 µL (0.16 µg/test)	Mouse cells (bone marrow)	Yes	BD Biosciences	741227
349 UV9	615/24	Brilliant Ultra Violet 615	CD11c	HL3	5 µL (1 µg/test)	Beads		BD Biosciences	751265
349 UV10	670/30	Brilliant Ultra Violet 661	CD93	AA4.1	1.2 µL (0.24 µg/test)	Beads	Yes	BD Biosciences	741574
349 UV12	750/LP	Brilliant Ultra Violet 805	B220	RA3-6B2	5 µL (1 µg/test)	Mouse cells (spleen)		Thermo Fisher Scientific	368-0452-82
405 V1	420/10	Brilliant Violet 421	Siglec-H	551	2.5 µL (0.5 µg/test)	Beads	Yes	BD Biosciences	567815
405 V3	455/14	eFluor 450	CD21	eBio4E3	5 µL (1 µg/test)	Beads	Yes	Thermo Fisher Scientific	48-0212-82
405 V5	507/19	Brilliant Violet 510	CCR2	475301	3 µL (0.6 µg/test)	Beads	Yes	BD Biosciences	747970
405 V7	575/15	Brilliant Violet 570	CD8	53-6.7	3 µL (0.6 µg/test)	Beads		BioLegend	100740
405 V8	615/24	Super Bright 600	I-A/I-E	M5/114.15.2	0.6 µL (0.12 µg/test)	Mouse cells (spleen)	Yes	Thermo Fisher Scientific	63-5321-82
405 V9	661/20	Brilliant Violet 650	Ly6G	1A8	1.25 µL (0.25 µg/test)	Mouse cells (bone marrow)		BioLegend	127641
405 V10	710/20	Super Bright 702	IgD	11-26c	2 µL (0.4 µg/test)	Beads		Thermo Fisher Scientific	67-5993-82
405 V11	747/33	Brilliant Violet 750	CD4	GK1.5	1.25 µL (0.25 µg/test)	Beads		BioLegend	100467
405 V12	770/LP	Super Bright 780	CD11b	M1/70	1.2 µL (0.24 µg/test)	Mouse cells (bone marrow)	Yes	Thermo Fisher Scientific	78-0112-82
445 VB1	465/22	Brilliant Violet 480	CD62L	MEL-14	0.3 µL (0.06 µg/test)	Beads	Yes	Thermo Fisher Scientific	414-0621-82
488 B1	507/19	FITC	TER-119	TER-119	1 µL (0.5 µg/test)	Beads		Thermo Fisher Scientific	11-5921-82
488 B2	549/15	LIVE/DEAD Fixable Olive	Dead cells		1:2,000	Mouse cells (spleen)		Thermo Fisher Scientific	L34978
488 B6	720/60	PerCP-eFluor 710	CD1d	1B1	0.75 µL (0.15 µg/test)	Beads	Yes	Thermo Fisher Scientific	46-0011-82
488 B7	750/LP	RealBlue 780	CD24	M1/69	1 µL (0.2 µg/test)	Mouse cells (bone marrow)	Yes	BD Biosciences	755892
561 Y1	575/15	PE	CD127	A7R34	2.5 µL (0.5 µg/test)	Beads	Yes	Thermo Fisher Scientific	12-1271-82
561 Y3	605/15	PE-eFluor 610	IgM	II/41	1.5 µL (0.3 µg/test)	Mouse cells (spleen)		Thermo Fisher Scientific	61-5790-82
561 Y5	661/20	PE-Cy5	CD3	17A2	5 µL (1 µg/test)	Beads		Thermo Fisher Scientific	15-0032-82
561 Y8	720/24	PE-Cy5.5	CD49b	DX5	0.75 µL (0.15 µg/test)	Beads	Yes	Thermo Fisher Scientific	35-5971-82
561 Y9	760/50	PE-Cy7	CD23	B3B4	1.2 µL (0.24 µg/test)	Beads	Yes	Thermo Fisher Scientific	25-0232-82
637 R1	670/30	APC	CD335	29A1.4	5 µL (1 µg/test)	Beads	Yes	Thermo Fisher Scientific	17-3351-82
637 R2	700/13	NovaFluor Red 700	CD45	30-F11	1.5 µL (0.15 µg/test)	Mouse cells (spleen)		Thermo Fisher Scientific	M005T02R03
637 R5	770/LP	APC-eFluor 780	Ly6C	HK1.4	2 µL (0.4 µg/test)	Mouse cells (bone marrow)		Thermo Fisher Scientific	47-5932-82

Gating strategy

Data cleanup and initial gating for populations of interest

Before identifying populations of interest for sorting and analysis, it is crucial to exclude from the data artifacts of sample and instrument processing. The first step in this gating strategy is to isolate singlets from doublets using side scatter area (SSC-A) versus side scatter height (SSC-H) parameters (Figure 2). Next, cell and tissue debris are further excluded by scatter gating, forward scatter area (FSC-A) versus SSC-A, followed by exclusion of dead cells that are stained with LIVE/DEAD Fixable Olive viability dye. Even though red blood cell lysis was performed during sample preparation, there is always a small percentage of erythroid cells that remain in the sample when lysis is performed as gently as possible. Therefore, the TER-119 marker is used to exclude remaining erythroid cells. All $CD45^+$ cells that are also $TER-119^-$ are selected to continue gating. Next, neutrophils are identified based on the positive expression of both Ly6G and Ly6C, and gating analysis is continued on the $Ly6G^-$ cells. $Ly6G^-$ cells are then separated based on their expression of Siglec-H and Ly6C for the identification of cellular subsets in the following sections. In several populations, the gating of positive vs. negative events was guided by previous experience with this panel and tissue types. For populations of reduced gating confidence, FMO samples were prepared and acquired under the same instrument conditions as samples (see Table 2 for detailed FMO listings).

Spleen pDCs, monocytes, DCs, and NK cells

From the population that is Siglec-H^+ $Ly6C^+$, plasmacytoid dendritic cells (pDCs) are confirmed by the positive expression of B220 and absence of CD11b (Figure 3).

Siglec-H^- $Ly6C^{hi}$ cells are further separated into $CD11b^+$ $CCR2^+$ cells, which identifies inflammatory monocytes (labeled as $CCR2^+$ monocytes).

Siglec-H^- cells that do not have high expression of Ly6C, though it may or may not be expressed, are further separated based on the expression of B220 and CD3, which identifies 3 different clusters: B lineage cells ($B220^+$), T cells ($CD3^+$), and $B220^-$ $CD3^-$ cells. From the $B220^-$ $CD3^-$ cells, DCs are identified based on the expression of CD11c and MHC class II (I-A/I-E) and are flagged for sorting. After excluding $CD11c^+$ and $MHCII^+$ cells, populations that express CD335 (Nkp46) and CD49b (natural killer (NK) cell markers that identify at least 2 different NK cell populations) are grouped together for sorting.

Spleen B cells

Spleen B cells are identified based on positive expression of B220 and CD19. To separate immature/transitional B cells from other subsets, CD24 and CD93 are used, where $CD24^{hi}$ $CD93^+$ gating identifies these cells (Figure 3). The immature/transitional cell group ($CD24^{hi}$ $CD93^+$) contains different transitional phenotypes that can be observed by analyzing the expression of CD23 and IgM. Different transitional B cells are identified by these characteristics: transitional 1 B (T1B, IgM^{hi} $CD23^-$), transitional 2 B (T2B, IgM^{hi} $CD23^+$), and transitional 3 B (T3B, $IgM^{-/low}$ $CD23^+$). T1B cells are selected as a target for sorting.

As for the other B cell subsets, $CD93^+$ cells are excluded from the gate and the expression of CD23 is considered. $CD23^+$ cells are further separated based on their positive expression of both IgM and IgD, which together identify mature IgM^+ B cells. From the $CD23^{-/low}$ gate, high expression of CD21 and CD1d identifies marginal zone B (MZB) cells, which are also selected for sorting.

Spleen T cells

Spleen T cells are identified based on $CD3^+$ expression and further separated into either $CD4^+$ or $CD8^+$ T cells (Figure 3). Regulatory T (Treg) cells are identified based on positive expression of CD25 and low or absent expression of CD127 from the $CD4^+$ T cell gate. These Treg cells are also a target for sorting in this experiment. After removing $CD25^+$ expression of the $CD4^+$ gate, the expression of CD62L and CD44 is used to identify 4 different T cell subsets, including naive ($CD62L^+$ $CD44^{-/low}$), central memory T (T_{CM}, $CD62L^+$ $CD44^+$), effector memory T (T_{EM}, $CD62L^-$ $CD44^+$), and effector T (T_{Eff}, $CD62L^-$ $CD44^-$). The same strategy based on CD62L and CD44 expression is used to identify the different $CD8^+$ T cell subsets from the $CD8^+$ gate, and $CD8^+$ naive T cells are selected as a target for sorting.

Spleen and bone marrow B cell comparison plots

Bone marrow is the major site of postnatal B cell development in both mice and humans. B cell precursors undergo step-by-step differentiation in the bone marrow until they form a functional B cell receptor that is expressed on the cell surface as IgM and functions as their antigen receptor. These newly generated IgM^+ B cells are identified as immature B cells, undergo further differentiation into transitional B cells that enter circulation, and complete their maturation in the spleen. Since this comprehensive immunophenotyping panel was applied in both bone marrow and spleen samples, a snapshot of B cell development can be made to compare the different B cell subsets found in either tissue.
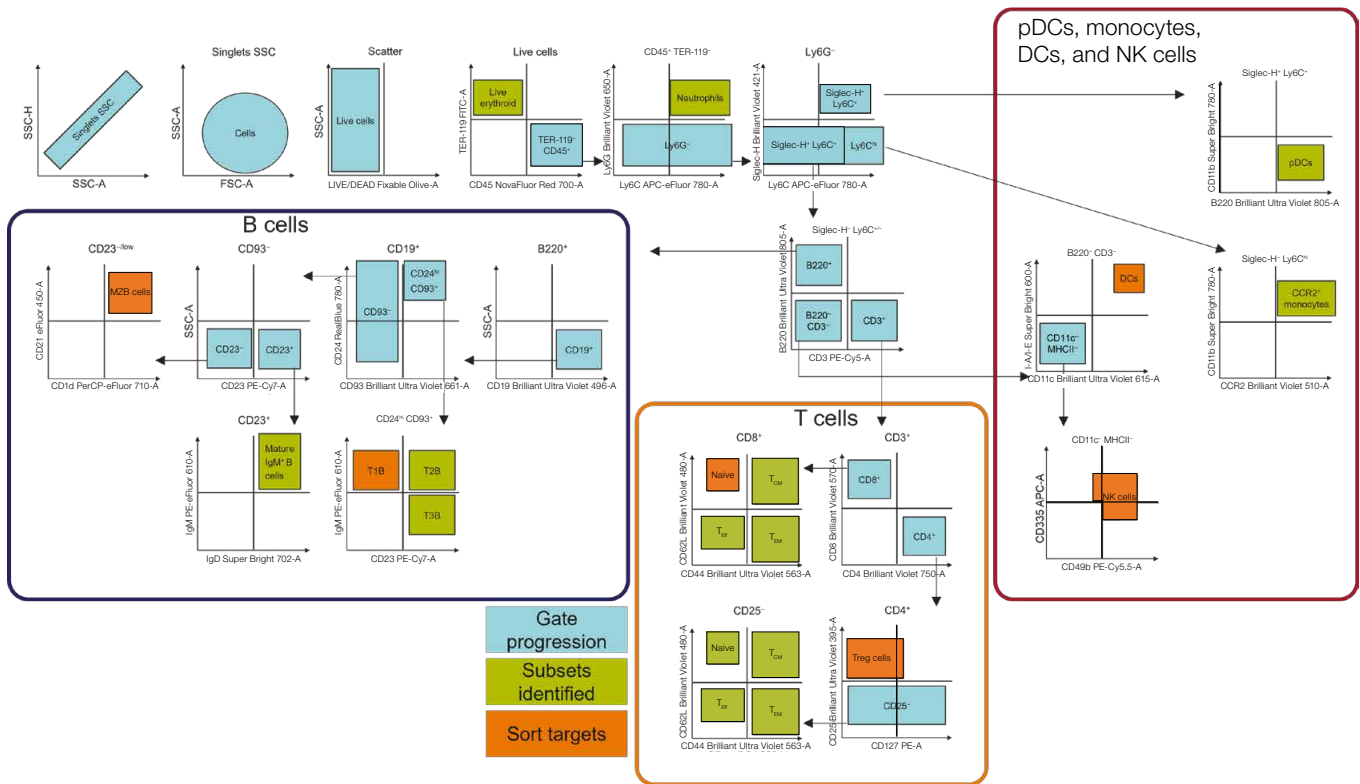
Figure 2. Gating layout for identifying and sorting spleen cells using a 28-color immunophenotyping panel. Sequential gate progression starts at the top from left to right and is depicted in blue. When more than one population is identified in the same plot, arrows are used to delineate gate progression for the different subpopulations. Green shapes represent the final gating strategy for the identified subsets, which include live erythroid cells, neutrophils, plasmacytoid dendritic cells (pDCs), CCR2$^+$ monocytes, central memory T (T$_{CM}$) cells, effector memory T (T$_{EM}$) cells, effector T (T$_{Eff}$) cells, transitional 2 B (T2B) cells, transitional 3 B (T3B) cells, and mature IgM$^+$ B cells. Orange shapes represent the 6 sort targets, which include dendritic cells (DCs), natural killer (NK) cells, regulatory T (Treg) cells, CD8$^+$ naive T cells, transitional 1 B (T1B) cells, and marginal zone B (MZB) cells.
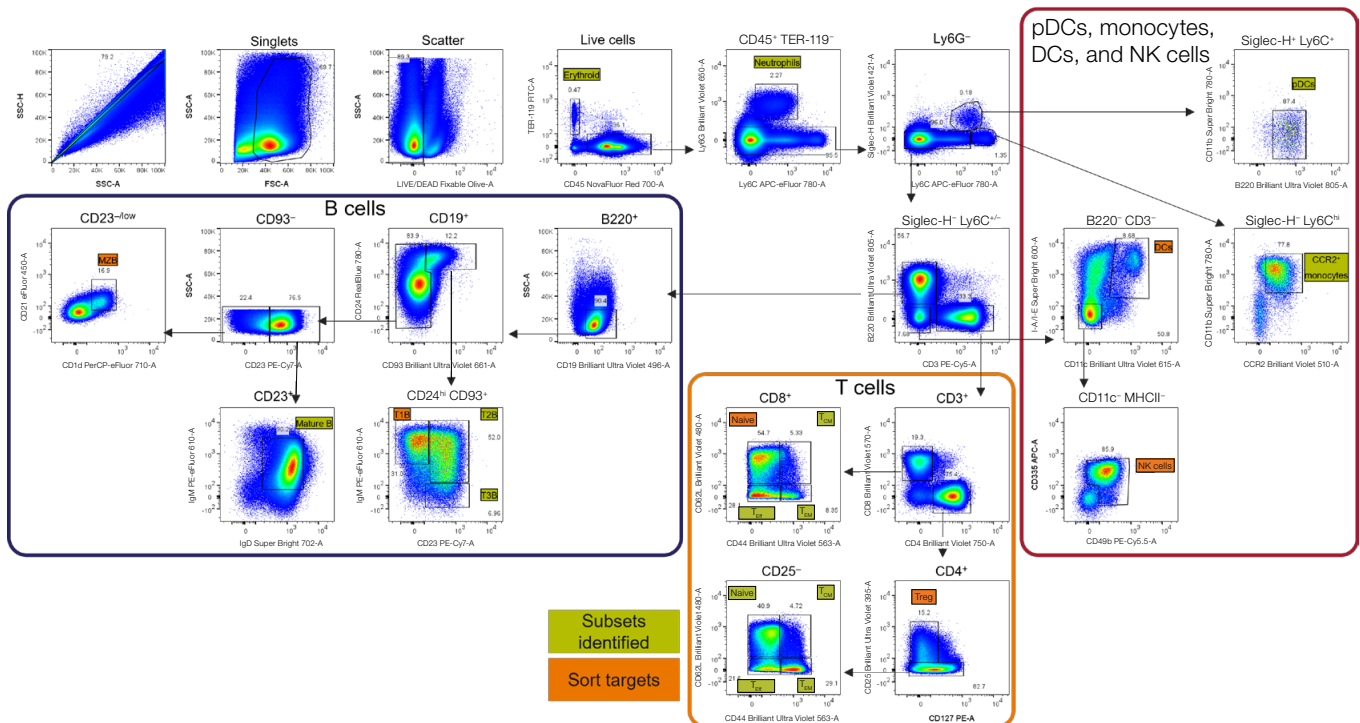
Figure 3. Cell gating for subset identification and sorting for the spleen sample. Sequential gate progression starts at the top and moves from left to right. When more than one population is identified in the same plot, arrows are used to delineate gate progression for the different subpopulations. Green shapes represent the final gating strategy for identified subsets, which include live erythroid cells, neutrophils, pDCs, CCR2$^+$ monocytes, T$_{CM}$ cells, T$_{EM}$ cells, T$_{Eff}$ cells, T2B cells, T3B cells, and mature IgM$^+$ B cells. Orange shapes represent the 6 sort targets, which include DCs, NK cells, Treg cells, CD8$^+$ naive T cells, T1B cells, and MZB cells.

As expected, most B cells in the bone marrow are identified as immature B cells (CD24^{hi} CD93$^+$ IgM$^+$ CD23$^-$), while the spleen has more mature B cells and fewer transitional subsets (Figure 4). The T2B cell subset can then differentiate into either follicular B cells or MZB cells that segregate to different areas of the spleen as their naming implies. The MZB cells reside only in the spleen and cannot be observed in the bone marrow.
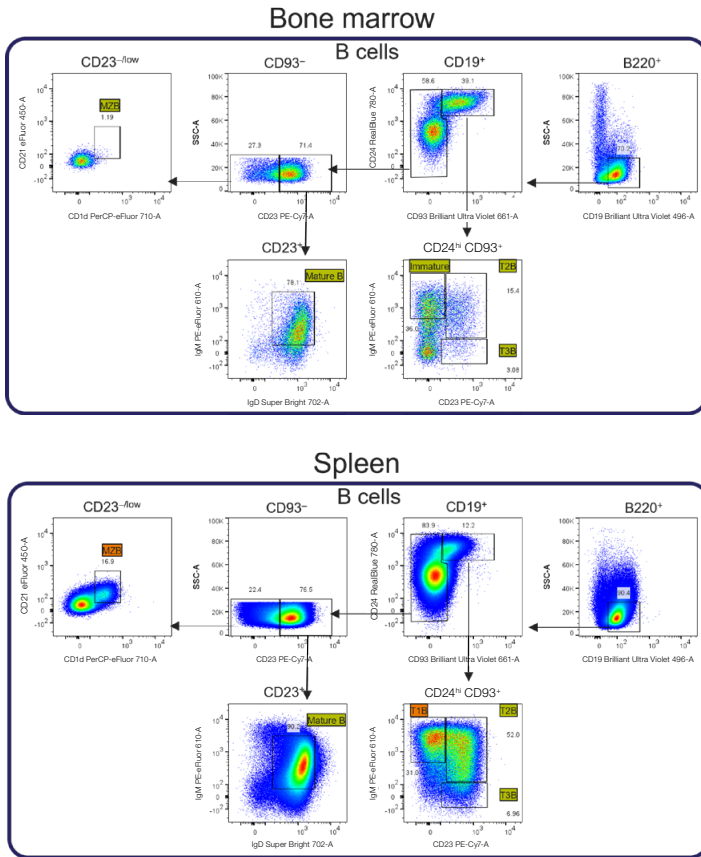
Figure 4. Comparison of B cell populations in bone marrow and spleen. The 28-color immunophenotyping panel applied to bone marrow and spleen tissues reveals different B cell maturation stages. Tissue specificities of transitional subsets serve as additional biological controls, confirming gating placements guided by the FMO controls. For example, bone marrow has an abundance of CD24^{hi} CD93$^+$ cells while MZB cells are absent, in contrast with the spleen.

Post-sort evaluation

Data analysis

Data analysis was performed with both FlowJo™ v10.9.1 Software (BD Biosciences) and GraphPad Prism™ 10.0.0 software (GraphPad Software).

Sorting efficiency

Efficiency is defined as the reported number of cells sorted by the cell sorter as a percentage of the number of target cells present in the sample. It is important to note that instrument manufacturers measure sorting efficiency differently. For a detailed examination of sorting efficiency, see the white paper "Bigfoot Cell Sorter: factors affecting efficiency, purity, and recovery" [6].

To robustly evaluate sorting efficiency using the approach detailed above, we evaluated efficiency across three separate experiments with the same target populations. The sort numbers varied within the three independent experiments due to the amount of sample available for staining, while the frequency of the sort targets within the sample was consistent (MZB cells = 1.5%, CD8$^+$ naive T cells = 2.5%, NK cells = 2.7%, Treg cells = 3.4%, T1B cells = 1.9%, and DCs = 0.38%). In each sample, the flow rate was adjusted as needed to maintain an event rate of 2,200–2,800 events per second during sorting. Figure 5 shows the efficiency results across these three experiments and highlights the consistency of this parameter.
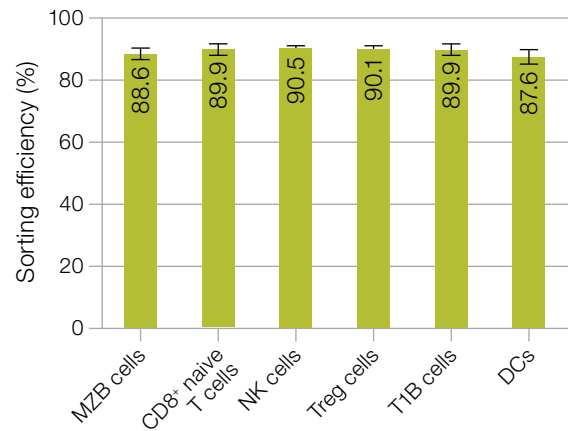
Figure 5. Sorting efficiency. Samples were acquired at a constant flow rate to maintain a speed of 2,200–2,800 events per second while sorting. Sorting priority index logic was based on the target population frequency in the spleen sample, with the less abundant events receiving the highest priority. DCs were less abundant in the spleen sample and were therefore placed in the right-3 position with the highest priority, followed by MZB cells placed in the left-3 position. T1B cells were placed in right-2, CD8$^+$ naive T cells in left-2, Tregs in right-1, and NK cells in left-1. Sorting efficiency is shown as the mean ± standard deviation of (percent sorted events) ÷ (percent aborted events) for 3 independent experiments.

Sorting recovery

In cell sorting, recovery refers to the proportion of desired cells in the sorted sample compared to the number the instrument indicates as sorted events. Recovery is an effective measure of sort performance since it considers the drop delay calculation and provides the actual yield of the isolation.

To calculate recovery after sorting, the total volume of sample was verified for each sorted tube by subtracting the weight of the empty tubes before the sort from the weight of the tubes after the sort. Following volume measurement, recovery was assessed by acquiring the sorted samples on the Attune NxT Flow Cytometer. The samples were gated on scatter and the cell concentration of each sample (events/µL) recorded.

Adjusted sorted cell numbers were obtained by multiplying the cell concentration by the sample volume. Lastly, the number of target cells in the sorted tube was divided by the number of target cells the instrument indicated it sorted. The calculated recovery percentages are displayed in Figure 6.

Purity determination

Purity is defined as the target cells found as a percentage of the total cell number in the sorted tube. Determination of post-sort purity requires a flow cytometric analysis of the collected sample, which was performed on the Bigfoot instrument (Figure 7).
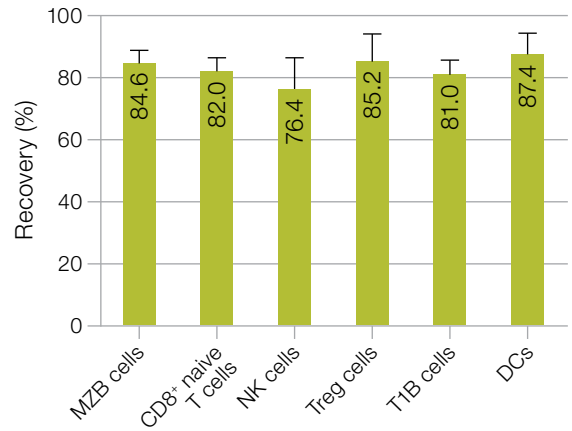
Figure 6. Percentage of cells sorted by the Bigfoot Cell Sorter that can be recovered for downstream analysis and applications. Recovery in cell sorting refers to the proportion of desired cells in the sorted sample compared to the number the instrument indicated as sorted events. Data are mean ± standard deviation for 3 independent experiments.
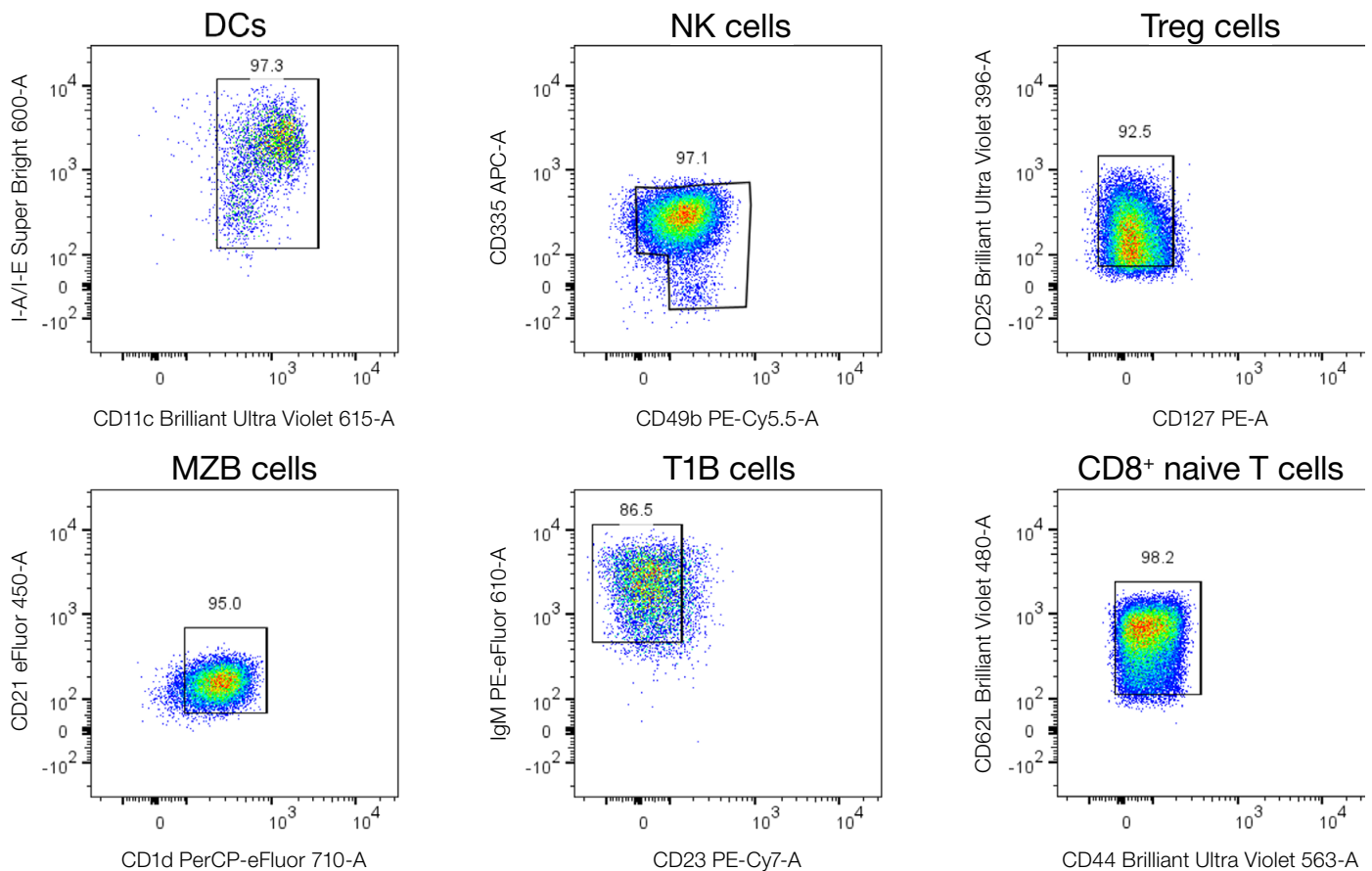
Figure 7. Purity check of sorted spleen cells. After sorting and assessing total sort numbers, the samples were rerun on the Bigfoot instrument for purity assessment. The gates were not adjusted for the post-sort purity assessment.

Conclusion

The Bigfoot Cell Sorter can resolve high-dimensional data by unmixing the spectral signatures of overlapping dyes. This allows greater panel expansion and consequently the amount of information that can be gathered from each sample. We have demonstrated that this 28-color panel can be used to identify up to 20 different populations from one sample. From those populations, the Bigfoot instrument can sort six ways, simultaneously, with high efficiency and purity, including several rare subsets from three tissue types.

Phenotypes used to identify mouse cell populations

- **Erythroid cells:** $CD45^-$ $TER-119^+$

- **Neutrophils:** $CD45^+$ $TER-119^-$ $Ly6C^+$ $Ly6G^+$

- **Plasmacytoid dendritic cells (pDCs):** $CD45^+$ $TER-119^-$ $Ly6G^-$ $Siglec-H^+$ $Ly6C^+$ $CD11b^-$ $B220^+$

- **CCR2$^+$ monocytes (inflammatory monocytes):** $CD45^+$ $TER-119^-$ $Ly6G^-$ $Siglec-H^-$ $Ly6C^{hi}$ $CD11b^+$ $CCR2^+$

- **Dendritic cells (DCs):** $CD45^+$ $TER-119^-$ $Ly6G^-$ $Siglec-H^-$ $B220^-$ $CD3^-$ $CD11c^+$ $MHCII^+$

- **Natural killer (NK) cells:** $CD45^+$ $TER-119^-$ $Ly6G^-$ $Siglec-H^-$ $B220^-$ $CD3^-$ $CD11c^-$ $MHCII^-$; $CD335^+$ $CD49b^+$ + $CD335^{-/low}$ $CD49b^+$ + $CD335^+$ $CD49b^{-/low}$

- **Regulatory T (Treg) cells:** $CD45^+$ $TER-119^-$ $Ly6G^-$ $Siglec-H^-$ $B220^-$ $CD3^+$ $CD4^+$ $CD127^{-/low}$ $CD25^+$

- **Naive T cells:** $CD45^+$ $TER-119^-$ $Ly6G^-$ $Siglec-H^-$ $B220^-$ $CD3^+$ [$CD4^+$ or $CD8^+$] $CD62L^+$ $CD44^{-/low}$

- **Central memory T (T$_{CM}$) cells:** $CD45^+$ $TER-119^-$ $Ly6G^-$ $Siglec-H^-$ $B220^-$ $CD3^+$ [$CD4^+$ or $CD8^+$] $CD62L^+$ $CD44^+$

- **Effector memory T (T$_{EM}$) cells:** $CD45^+$ $TER-119^-$ $Ly6G^-$ $Siglec-H^-$ $B220^-$ $CD3^+$ [$CD4^+$ or $CD8^+$] $CD62L^-$ $CD44^{+/hi}$

- **Effector T cells:** $CD45^+$ $TER-119^-$ $Ly6G^-$ $Siglec-H^-$ $B220^-$ $CD3^+$ [$CD4^+$ or $CD8^+$] $CD62L^-$ $CD44^{-/low}$

- **Transitional 1 B (T1B) cells:** $CD45^+$ $TER-119^-$ $Ly6G^-$ $Siglec-H^-$ $B220^+$ $CD3^-$ $CD19^+$ $CD24^{hi}$ $CD93^+$ IgM^{hi} $CD23^-$

- **Transitional 2 B (T2B) cells:** $CD45^+$ $TER-119^-$ $Ly6G^-$ $Siglec-H^-$ $B220^+$ $CD3^-$ $CD19^+$ $CD24^{hi}$ $CD93^+$ IgM^{hi} $CD23^+$

- **Transitional 3 B (T3B) cells:** $CD45^+$ $TER-119^-$ $Ly6G^-$ $Siglec-H^-$ $B220^+$ $CD3^-$ $CD19^+$ $CD24^{hi}$ $CD93^+$ $IgM^{-/low}$ $CD23^+$

- **Mature IgM$^+$ B cells:** $CD45^+$ $TER-119^-$ $Ly6G^-$ $Siglec-H^-$ $B220^+$ $CD3^-$ $CD19^+$ $CD93^-$ $CD23^+$ IgM^+ IgD^+

- **Marginal zone B (MZB) cells:** $CD45^+$ $TER-119^-$ $Ly6G^-$ $Siglec-H^-$ $B220^+$ $CD3^-$ $CD19^+$ $CD93^-$ $CD23^{-/low}$ $CD1d^+$ $CD21^+$

References

1. Andrä I, Ulrich H, Dürr S et al. (2020) An evaluation of T-cell functionality after flow cytometry sorting revealed p38 MAPK activation. *Cytometry* 97:171–183.
2. Richardson GM, Lannigan J, Macara IG (2015) Does FACS perturb gene expression? *Cytometry A* 87:166–175.
3. Box A, DeLay M, Tighe S et al. (2020) Evaluating the effects of cell sorting on gene expression. *J Biomol Tech* 31:100–111.
4. Beliakova-Bethell N, Massanella M, White C et al. (2014) The effect of cell subset isolation method on gene expression in leukocytes. *Cytometry* A 85:94–104.
5. Cochran M, Bergeron A, Box A et al. (2015) Evaluating the effects of cell sorting on gene expression. Paper presented at the Association of Biomolecular Resource Facilities conference, Salt Lake City, Utah, USA 2015.
6. Thermo Fisher Scientific. Bigfoot Cell Sorter: factors affecting efficiency, purity, and recovery. White paper on **thermofisher.com**

Learn more at **thermofisher.com/bigfoot**

invitrogen